Journal of Environmental Chemical Engineering 5 (2017) 2222–2231

Contents lists available at ScienceDirect

Journal of Environmental Chemical Engineering

journal homepage: www.elsevier.com/locate/jece

Adsorption of 2,4-dichlorophenol on paper sludge/wheat husk biochar: Process optimization and comparison with biochars prepared from wood chips, sewage sludge and hog fuel/demolition waste

Dimitrios Kalderis[a,*], Berkant Kayan[b], Sema Akay[b], Esra Kulaksız[b], Belgin Gözmen[c]

[a] Department of Environmental and Natural Resources Engineering, School of Applied Sciences, Technological and Educational Institute of Crete, Chania, Crete, Greece
[b] Department of Chemistry, Arts and Science Faculty, Aksaray University, Aksaray, Turkey
[c] Department of Chemistry, Arts and Science Faculty, Mersin University, Mersin, Turkey

ARTICLE INFO

Keywords:
2,4-dichlorophenol
Chlorophenols
Biochar
Adsorption
Biomass pyrolysis

ABSTRACT

The adsorption of 2,4-dichlorophenol, a toxic by-product of triclosan commonly found in wastewater treatment plant effluents, was studied on paper sludge/wheat husks biochar. By using response surface methodology, the optimum conditions and effects of pH, temperature, initial 2,4-DCP concentration and time were determined. The solution pH was found to be the most influential parameter whereas the optimum adsorption conditions were predicted as: C_0 = 40.28 mg L^{-1}, T = 326 K, pH = 2.8, t = 143 min, where a 99.95% adsorption could be achieved. Both Langmuir and Freundlich provided a good fit for the experimental data, indicating a surface and multi-layer adsorption. Kinetically, the process primarily followed the pseudo-second order model (chemisorption). By comparing the adsorption capacity at equilibrium of our main biochar (q_e = 9.28 mg g^{-1}) to 3 biochars prepared from different biomasses (q_e values 1.57–2.96 mg g^{-1}), it was concluded that pH-dependent electrostatic interactions and non-covalent π-electron donor-acceptor mechanisms play the most important role. Finally, there was indication that high concentrations of Ca and K may promote the adsorbate-adsorbent interactions and enhance adsorption.

1. Introduction

Triclosan (TCS, 5-chloro-2-(2,4-dichlorophenoxy)phenol) is a common antifungal and antibacterial agent added for many decades in products such as toothpastes, detergents and healthcare consumables. The use of these products results in triclosan-containing wastewaters, which are conventionally treated in municipal wastewater treatment plants. Approximately, 97–98% of triclosan is degraded or precipitated during treatment, however there are still substantial quantities released in the environment through effluent discharge. The endocrine disrupting activity of triclosan and its aquatic toxicity have been well documented [1–3].

Various dioxins, chlorinated/hydroxylated diphenyl ethers and chlorophenols are the main by-products of Triclosan's aerobic degradation [4,5]. One of the most recalcitrant and frequently occurring degradation product is 2,4-dichlorophenol (2,4-DCP). This by-product is known to have adverse effects to both microorganisms and certain functions of the human body. Studies have shown that it restricts freshwater algal growth [6], the vegetative reproduction of the duckweed (*Lemna gibba*) [7] and shows acute toxicity to the brine shrimp *Artemia sinica* (Artemia) [8]. Furthermore, the endocrine disrupting effect of 2,4-DCP on reproductive and thyroid hormones has been established [9]. Additionally, the substance has been linked to reduced head circumference and birth weight to newborns [10] whereas its long-term exposure pathway targets the nervous system, liver and kidneys [11].

There are several biological, chemical and physical methods that can effectively degrade or remove 2,4-DCP and other chlorophenols from water and wastewater. For many of them, one common degradation route is catalytic dechlorination. Zhou et al. successfully used a bimetallic Au-decorated Pd catalyst, whereas Cui et al. showed that N-doped, carbon-supported nanoparticles can help achieve a nearly 100% conversion of 2,4-DCP to phenol [12,13]. After 3hr of treatment at pH 6, the same conversion rate was achieved by Xu et al., who used Ni/Fe-Fe_3O_4 nanocomposites [14]. Other nanoscale materials that have been tested include calcium peroxide [15] and $Ce_xFe_{1-x}O_2$ composite [16].

Several other researchers have investigated 2,4-DCP degradation through advanced oxidation processes. Notably, pre-magnitized Fe^0

* Corresponding author.
E-mail addresses: dkalderis@chania.teicrete.com (D. Kalderis), berkantkayan@gmail.com (B. Kayan), sema.akay7@gmail.com (S. Akay), esra_kulaksiz@hotmail.com (E. Kulaksız), bgozmen@yahoo.com (B. Gözmen).

http://dx.doi.org/10.1016/j.jece.2017.04.039
Received 18 December 2016; Received in revised form 20 March 2017; Accepted 21 April 2017
Available online 24 April 2017

promoted the production of ·OH radicals, which in turn attacked and oxidized 2,4-DCP [17]. In addition to ·OH, free radicals such as $SO_4\cdot^-$, $HO_2\cdot$ and MnO_4^- have been extensively used in the past for chlorophenol degradation [[18] and references therein]. Using an inexpensive Fe-C catalyst modified with polytetrafluoroethylene, Zhan et al. degraded 2,4-DCP and established the feasibility of the electro-Fenton method they followed, under neutral conditions [19]. However, when the authors used real industrial wastewaters spiked with 2,4-DCP, they found that its removal rate was lower, probably due to competitive reactions of other organics with the hydroxyl radical. Other effective advanced oxidation set-ups include the use of UV light in combination with boron-doped TiO_2 [20] and Pd-Fe/graphene photocatalysts to eliminate 2,4-DCP from aqueous samples [21].

Adsorption methods have been traditionally used to remove hazardous substances from water and wastewater. Yang et al. added dealuminated zeolites to various chlorophenol solutions and concluded that sorption was improved as the hydrophobicity of the substance was increased and in the presence of metal cations [22]. The beneficial effect of metal cations on 2,4-DCP adsorption was confirmed by Ortiz-Martinez et al. who used Ni^{2+}, Cu^{2+} or Co^{2+} loaded on natural clay [23]. The authors concluded that the rate-determining steps were hydrogen bond formation, complexation with the metal and hydrophobic interactions. Simsek et al. compared cellulose-based microporous carbon fibers of different surface areas and found that at pH 6, the fiber with the highest surface area achieved the highest 2,4-DCP removal [24].

The conversion of agricultural or other bio-waste to added-value materials for the treatment of 2,4-DCP containing wastewaters has not been thoroughly investigated. A range of activated carbons have been tested [25–28] but they showed certain disadvantages, such as multiple preparation steps, relatively slow contaminant uptake and often poor regeneration behavior [29]. Biochar is the carbonaceous product of biomass pyrolysis. It can be prepared from a wide range of biomasses, from sewage sludge to rice husks and other agricultural residues. It possesses several soil improving properties (depending on feedstock and pyrolysis conditions) therefore considerable amount of biochar research involves soil applications [30,31]. However, in many cases it has proven as efficient adsorbent as activated carbon for both inorganic and organic contaminants without the need for an additional activation step [32–34]. Most researchers have focused on heavy metal adsorption on biochars, whereas the studies involving adsorption of persistent organics and in particular endocrine-disrupting substances are only a few.

The rationale behind this work was to develop a simple methodology for efficient adsorption of 2,4-DCP from aqueous solutions based on a biochar produced from abundant waste materials, thus avoiding the use of costly activated adsorbents. Additionally, further knowledge on the adsorption mechanisms involved will allow researchers to focus on specific biomass properties and pyrolysis conditions towards purpose-prepared biochars. Therefore, we investigated and optimized the adsorption of 2,4-DCP on biochar prepared from a mixture of paper sludge and wheat husks. By applying the Box-Behnken experimental design as part of a response surface methodology (RSM), the process was optimized and the interactive effects of pH, initial 2,4-DCP concentration, temperature and time were determined. Adsorption was mechanistically studied by applying our experimental data to known isotherm and kinetic models. Finally, the optimum adsorption conditions obtained with the paper sludge/wheat husk biochar sample were applied to three fundamentally different biochars and the adsorption capacities at equilibrium were compared.

2. Materials and methods

2.1. Materials

The equilibrium adsorption, kinetic studies and the subsequent optimization were performed on paper sludge/wheat husks biochar obtained from Sonnenerde GmbH (Riedlingsdorf, Austria). The sample was used as received without washing or any other processing/modification (coded BC-A thereafter). Three more biochar samples, namely wood chip biochar (Swiss Biochar, Lausanne, Switzerland), sewage sludge biochar (Pyreg GmbH, Dörth, Germany) and hog fuel/demolition waste biochar (Olympic Biochar, Port Townsend, USA) were used to compare the 2,4-DCP adsorption rate at the optimum conditions. These samples were coded BC-B, BC-C and BC-D, respectively. Based on preliminary experiments, the optimization of adsorption was based on BC-A. All biochars were sieved to a particle size of < 250 μm (60 mesh) before use. The production conditions and characterization of all samples can be seen in Table 1. BC-A was morphologically characterized in a Zeiss/Supra 55 (Germany) high-resolution scanning electron microscope (SEM). The sample was coated with platinum/palladium by electro deposition under vacuum prior to analysis to enhance the surface conductivity. Energy-dispersive X-ray (EDX) spectroscopy analysis was performed on BC-A after adsorption, using a Quantax instrument (Bruker, USA). The surface chemistry of all adsorbents was investigated further, through the determination of the pH point of zero charge (pH_{pzc}). At pH values above the zero point charge, the surface of the adsorbent has a net negative or anionic charge, and it would promote cation attraction, and cation exchange reactions. At pH values below the zero point charge, the surface has a net positive charge, it will attract anions and consequently participate in anion exchange reactions. The pH_{pzc} was determined using the methodology described in Newcombe et al. [35]. 2,4-DCP was obtained from Sigma-Aldrich (Germany). Fourier-Transform Infrared (FTIR) analysis of biochar samples before and after treatment, was recorded using a Perkin Elmer Model FTIR Frontier spectrophotometer with attenuated total reflection (ATR) technique in the 4000–500 cm^{-1} region.

Table 1
Characterization of the biochar samples and properties of 2,4-DCP.

	BC-A	BC-B	BC-C	BC-D
Production temperature/°C	500	620	600	600
Residence time/min	20	20	20	nr[a]
Total C (%)	50.5	81.2	18.7	80.7[b]
H (%)	1.55	1.19	0.93	2.2
N (%)	1.29	0.42	2.1	0.97
O (%)	6.4	3.8	3.7	9.6
S (%)	0.14	–	0.76	nr
O/C ratio	0.126	0.046	0.197	0.118
Ash content (%)	40.2	13.3	73.3	6.5
P (mg kg^{-1})	6610	870	61500	683
K (mg kg^{-1})	16800	9400	10300	2869
Na (mg kg^{-1})	910	690	4140	680
Mg (mg kg^{-1})	4530	2320	13300	nr
Mn (mg kg^{-1})	127	301	514	414
Ca (mg kg^{-1})	89200	33700	54400	nr
Fe (mg kg^{-1})	2780	1840	48000	1581
pH	8.3	8.3	7.1	8.4
Conductivity (μS cm^{-1})	759	989	617	114
Surface area (m^2 g^{-1})	63.8	224.8	25.6	360
pH_{pzc}	8.5	9.5	7.3	9.0
	2,4-dichlorophenol (2,4-DCP)			
Chemical formula	$C_6H_4Cl_2O$			
Molecular weight	163			
$LogK_{ow}$	3.2			
pK_a	7.89			
Water solubility (mg L^{-1})	4500			

[a] nr stands for not-reported.
[b] measurement is for organic carbon.

2.2. 2,4-DCP adsorption studies

A stock 2,4-DCP solution of 100 mg L^{-1} was prepared with distilled

water. Working solutions at the appropriate concentrations were prepared from the stock solution. The basic steps of the adsorption process are described in detail in Agrafioti et al. [36]. The adsorption percent was calculated as follows:

$$Adsorption\% = \frac{C_0 - C_e}{C_0} x100 \quad (1)$$

Where C_0 and C_e correspond to the initial concentration and the concentration after equilibrium, respectively (mg L^{-1}). The data obtained were fitted into the Langmuir and Freundlich isotherms in order to investigate the contaminant-surface interactions in more depth.

The process was optimized and the effect of initial 2,4-DCP concentration (20–60 mg L^{-1}), pH (2–10), temperature (303–333 K) and time (60–180 min) was investigated (labeled as X_1, X_2, X_3 and X_4, respectively). For this purpose, a three-level Box-Behnken response surface design was developed (Design Expert software). The above four independent variables (k) were studied at the low and high end of the experimental range as well as in midpoints. The Box-Behnken experimental design (BBD), developed by Box and Behnken in 1980, is a convenient method for improving second-order response surface models. Indeed, Box-Behnken is formed by combining two-level factorial designs with incomplete block designs. In this case, the designs with desirable statistical properties can be developed. It is enough to make only a fraction of the experiments required for a three-level fractional design to develop second degree models. A BBD should consist of an equal number of replicates of all possible combinations of factor levels. Experiments are performed at the equatorial distance from the central point of the hypercube and at the central point (N = 2k(k − 1) + cp). The results were a total of 29 experimental runs, the details of which are shown in Table 2. The adsorption% of 2,4-DCP was set as the response (Y). A water bath fitted with a temperature controller was used to control the experimental temperature where needed. Appropriate volumes of 0.1 M HCl or NaOH were used to adjust the pH at the required values. The residual 2,4-DCP concentration was measured using a UV–vis spectrophotometer at an absorbance wavelength of 280 nm.

Table 2
BBD with the experimental and predicted adsorption values for 2,4-DCP.

Run[a]	X_1 [2,4-DCP]$_0$	X_2 Temp.	X_3 pH	X_4 Time	Experimental adsorption%	Predicted adsorption %
1	20	303	6.00	120	90.74	91.68
2	60	303	6.00	120	81.73	82.60
3	20	333	6.00	120	91.85	91.50
4	60	333	6.00	120	86.73	86.31
5	40	318	2.00	60	93.50	93.77
6	40	318	10.00	60	62.17	62.82
7	40	318	2.00	180	97.96	97.49
8	40	318	10.00	180	65.95	66.54
9	20	318	6.00	60	86.55	87.08
10	60	318	6.00	60	78.03	79.94
11	20	318	6.00	180	89.21	90.79
12	60	318	6.00	180	80.83	83.65
13	40	303	2.00	120	94.96	95.47
14	40	333	2.00	120	98.85	101.11
15	40	303	10.00	120	67.22	68.39
16	40	333	10.00	120	63.37	66.29
17	20	318	2.00	120	98.79	98.13
18	60	318	2.00	120	91.53	89.63
19	20	318	10.00	120	67.85	65.81
20	60	318	10.00	120	63.33	60.05
21	40	303	6.00	60	89.05	87.60
22	40	333	6.00	60	90.15	88.23
23	40	303	6.00	180	92.20	90.18
24	40	333	6.00	180	95.57	93.08
25	40	318	6.00	120	91.55	91.37
26	40	318	6.00	120	92.02	91.37
27	40	318	6.00	120	90.73	91.37
28	40	318	6.00	120	93.07	91.37
29	40	318	6.00	120	91.36	91.37

[a] In all runs, 4 g adsorbent/L of working solution was used.

The experimental data obtained were fitted into a polynomial second degree model described by the following equation:

$$Y = \beta_0 + \sum_{i=1}^{k} \beta_i X_i + \sum_{i=1}^{k} \beta_{ii} X_i^2 + \sum_i \sum_j \beta_{ij} X_i X_j + \varepsilon \quad (2)$$

where, Y is the predicted response, X_i and X_j indicate the independent variables, ε represents the random error, β_o, β_i, β_{ii} and β_{ij} are the constant coefficient, the linear coefficient, the quadratic coefficient and the interaction coefficient, respectively.

The success of the model obtained − after the experimental results were entered into the BBD − was analyzed by analysis of variance (ANOVA). The R^2 and adjusted R^2 coefficient values correlated the experimental results to the theoretical results predicted by the model. Pareto chart analysis was used to examine the effect of each variable with linear and quadratic interactions on the response.

2.3. Study of adsorption kinetics

Kinetics were examined near the optimum pH value determined earlier through the equilibrium experiments. Briefly, 40 mg L^{-1} solutions were prepared from the stock and the residual 2,4-DCP concentration was monitored at time intervals of 10, 30, 60, 90, 120, 150 and 180 min at pH 2.8, whereas 4 g of adsorbent per liter of solution was used. The technical details of the process are described comprehensively in Agrafioti et al. [36]. The contaminant sorption per unit weight of adsorbent (q_t) was determined through the following equation:

$$q_t = \frac{V(C_0 - C_e)}{m} \quad (3)$$

Where, V corresponds to the volume of each 2,4-DCP working solution, C_e and C_o are the equilibrium and initial concentration respectively, and m is the dry weight of the adsorbent. Reproducibility was ensured by performing each kinetic experiment in triplicate. The mean values for q_t provided the basis for the data input in four commonly used kinetic models, the pseudo-first order, pseudo-second order, the intra-particle diffusion and Bangham models.

3. Results and discussion

3.1. Adsorption efficiency and validation of the proposed model

The experimental adsorption % values for 2,4-DCP can be seen in Table 2. At the conditions provided by the Box-Behnken design, adsorption ranged from 62.2 to 98.85%. The lowest adsorption % was found at a temperature of 318 K, treatment time of 60 min, initial contaminant concentration of 40 mg L^{-1}, and pH 10. The highest was achieved at a temperature of 333 K, treatment time of 120 min, initial contaminant concentration of 40 mg L^{-1}, and pH 2. Therefore, BC-A was successful in adsorbing 2,4-DCP within the experimental boundaries set by the Box-Behnken design. The SEM images revealed important information and morphological characteristics of BC-A before and after adsorption. Fig. 1(a) shows the rough surface of BC-A before adsorption, whereas images (b) and (c) clearly show a more uniform biochar surface covered in 2,4-DCP clusters with average size of ~120 nm. The EDX analysis (Fig. 2) confirmed the presence of 2,4-DCP on biochar through the presence of Cl atoms (2.6 keV).

The experimental data provided the input for the polynomial second degree model described earlier (Eq. (2)). After processing (Design Expert software), the empirical relationship between the adsorption% and the four variables (and the interactions between them) was developed and is shown below:

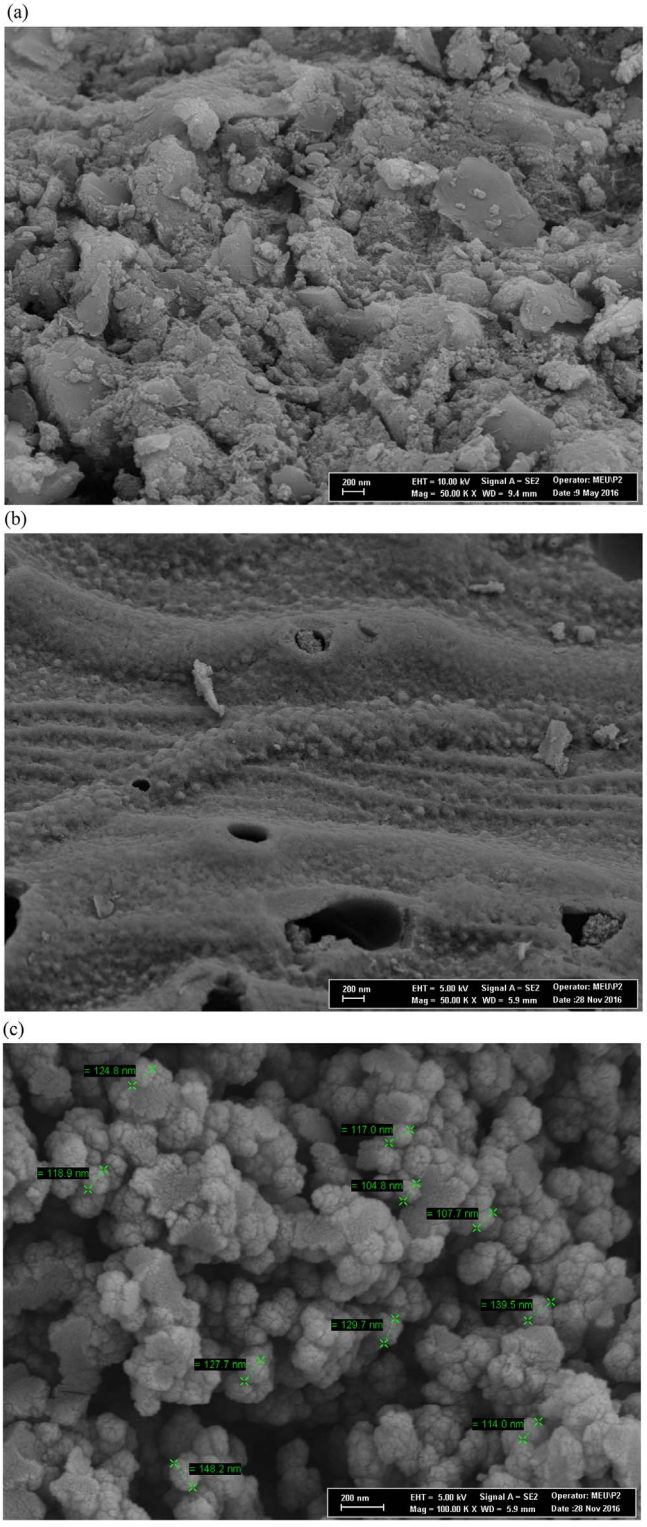

Fig. 1. SEM images of BC-A before (a) and after (b)–(c) adsorption at the 200 nm scale.

$$Y\,(Adsorption\%) = 91.75 - 3.57X_1 + 0.88X_2 - 15.48X_3 + 1.86X_4 + 0.97X_1X_2 + 0.69X_1X_3 - 1.93X_2X_3 + 0.57X_2X_4 - 4.07X_1^2 + 0.34X_2^2 - 9.28X_3^2 - 2.32X_4^2 \quad (4)$$

The Pareto chart was also used to show the significant variables for response and is provided in Fig. 3. The percentage effect of each of the last six factors was below 1%. The positive or negative effect of each factor on the response were marked on the graph as + or − signs, respectively. Both Eq. (4) and the Pareto chart showed that pH (X_3) had a significant linear (65%) and quadratic (23%) effects in negative direction. Following pH was the initial 2,4-DCP concentration (X_1), which again showed a negative correlation. The linear and quadratic percentage effect values for this factor were 3.4% and 4.5%, respectively. The adequacy of the proposed regression model and the statistical significance of each term were examined and the results are presented in Table 3. The comparison of the calculated F-value for the model (70.46) to the tabulated F-value ($F_{0.05,12,16} = 2.42$) indicated that overall the model was highly significant and adequately described the adsorption process. It is known that if the calculated F value is considerably higher than the tabulated F value, then the proposed model can successfully predict the Y response (adsorption) within the system's boundaries [37]. Additionally, the overall probability value of < 0.0001 confirmed the above conclusion. The higher the F-values and the lower the p-values are, the greater the effect of each variable in the process [38].

Therefore, in our case the following parameters were the most influential (in order of decreasing significance): pH > initial 2,4-DCP concentration > time > temperature. Among the quadratic terms, the term X_3^2 that corresponds to pH shows the higher F-value (126.3, p-value < 0.0001). The quality of the fit of the model was also expressed by the correlation coefficient (R^2) of 0.9814 which is used to check the correlation between the experimental data and predicted responses. At the same time, the adjusted coefficient (R^2_{adj}) of 0.9675 indicated the model's success to compare the influence of each independent variable. The coefficient of variance (C.V.) was determined as 2.46, indicating high precision and very reliable data.

Within the experimental range for each variable and by setting 80% as the minimum acceptable adsorption %, the optimum parameters were determined as 40.28 mg L^{-1} 2,4-DCP concentration, pH 2.81, temperature 326 K, and treatment time 143 min, where 99.95% adsorption efficiency could be achieved with a desirability value of 1.00.

3.2. Synergies between the process variables

Based on Eq. (4), three dimensional response plots were drawn. These plots illustrated the effect of initial 2,4-DCP concentration, temperature, pH and time on adsorption % of 2,4-DCP on biochar (Fig. 4). The combined effect of temperature and initial concentration on adsorption, while holding other variables constant, is shown in Fig. 4a. At any contaminant concentration, raising the temperature by 30 K only increased adsorption by approximately 5%. This observation confirmed the earlier finding that temperature was the least influential factor and that the process is endothermic. Ren et al. improved the adsorption of 2,4-DCP by modified phoenix tree leaves by 16%, when they raised the temperature by 20 K. The extent to which temperature affects the process is mainly based on the diffusion of the molecules to the internal pores of the adsorbent [39]. This mechanism becomes more important in adsorbents with high surface area and well-developed microporous structure not typically found in biochars. In our case, it is more likely that the small increase in adsorption was the result of H-bonding breaking between 2,4-DCP and water. This would cause 2,4-DCP to be less soluble in water and show a greater affinity for the biochar surface [26,40].

As expected, increasing 2,4-DCP concentration from 20 to 60 mg/L, resulted in ~15% reduction in adsorption. This is typically observed in the adsorption of both inorganic and organic species by carbonaceous materials [[37,41] and references therein] and is due to the saturation of the available sorption sites on the adsorbent surface [42].

Fig. 4b presents the effect of initial 2,4-DCP concentration and pH on the adsorption efficiency of biochar (at constant treatment time and temperature). Regardless of concentration, the highest adsorption% was achieved at pH 2. The effect of pH is so decisive that reducing or increasing the concentration had comparably a negligible effect on

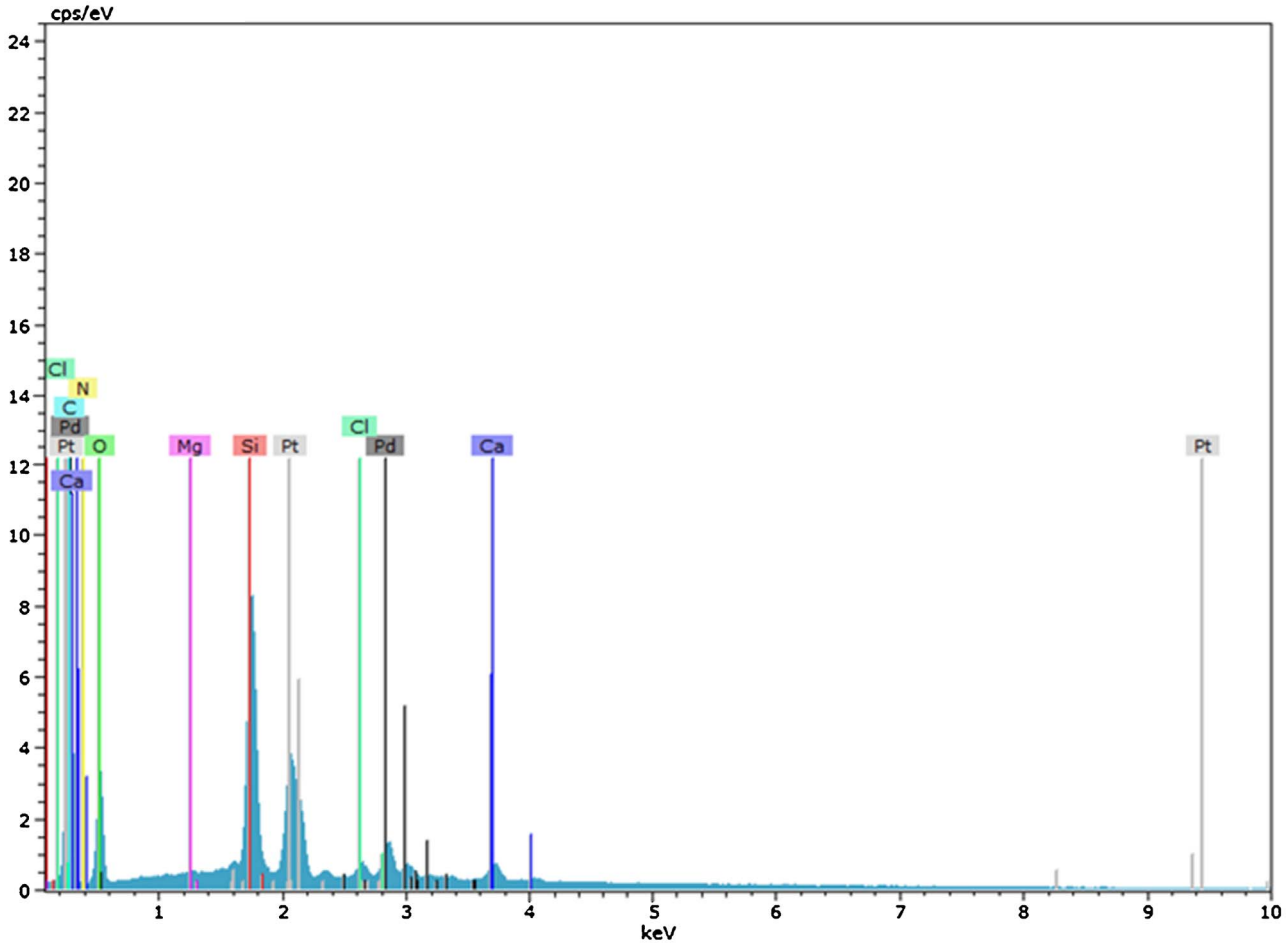

Fig. 2. EDX spectrum of BC-A after adsorption.

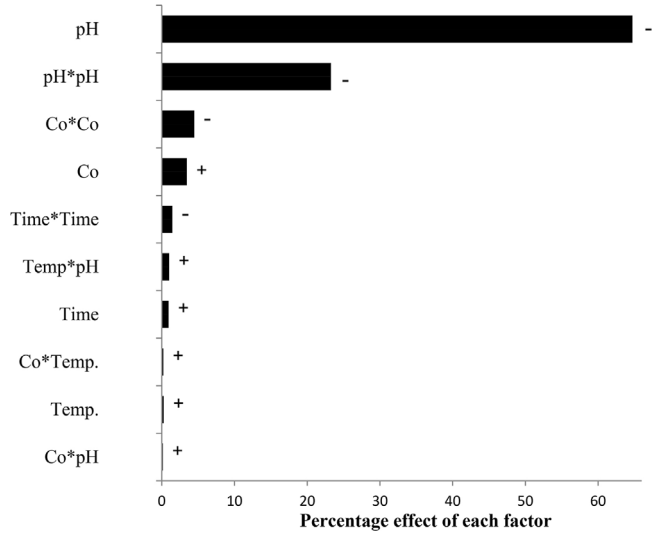

Fig. 3. Pareto graphic analysis (The positive or negative effect of each factor on the response were marked on the graph as + or − signs, respectively).

Table 3
Analysis of variance results for the validation of the quadratic model proposed.

Source	SS[a]	df[b]	MS[c]	F-value	P-value
Model	3737.02	12	311.42	70.46	< 0.0001
X_1-[2,4-DCP]$_0$	152.72	1	152.72	34.56	< 0.0001
X_2-Temperature	9.40	1	9.40	2.13	0.1641
X_3-pH	2873.71	1	2873.71	650.21	< 0.0001
X_4-Time	41.33	1	41.33	9.35	0.0075
X_1X_2	3.78	1	3.78	0.86	0.3686
X_1X_3	1.88	1	1.88	0.42	0.5239
X_2X_3	14.98	1	14.98	3.39	0.0843
X_2X_4	1.29	1	1.29	0.29	0.5967
X_1^2	107.19	1	107.19	24.25	0.0002
X_2^2	0.75	1	0.75	0.17	0.6849
X_3^2	558.16	1	558.16	126.29	< 0.0001
X_4^2	34.77	1	34.77	7.87	0.0127
Residual	70.71	16	4.42		
Lack of Fit	67.67	12	5.64	7.40	0.0338
Pure error	3.05	4	0.76		
Correlation total	3807.74	28			
Adeq Precision 29.558	29.17				

[a] Sum of Squares.
[b] Degree of Freedom.
[c] Mean Square.

adsorption. The dominant effect of pH was also confirmed in Fig. 4c. A pH value of 2 appeared again as the optimum, regardless of temperature. The effect of the solution pH on 2,4-DCP adsorption on activated carbons and other sorbents has been extensively studied and several researchers have determined a pH range between 2 and 3 as the optimum [24,39,42–44]. The solution pH determines to a large extent which form 2,4-DCP takes in solution: at a pH value below 6, the non-dissociated form of the substance prevails, whereas at pH > 9 the deprotonated (dichlorophenate) form accounts for more than 95% of all the 2,4-DCP present. Wang et al. used activated carbon fibers from polyvinyl alcohol to remove 2,4-DCP from aqueous solutions. The authors obtained their maximum adsorption capacity (396.3 mg g^{-1}) and best Langmuir correlation coefficient of 0.990 at pH 3 and

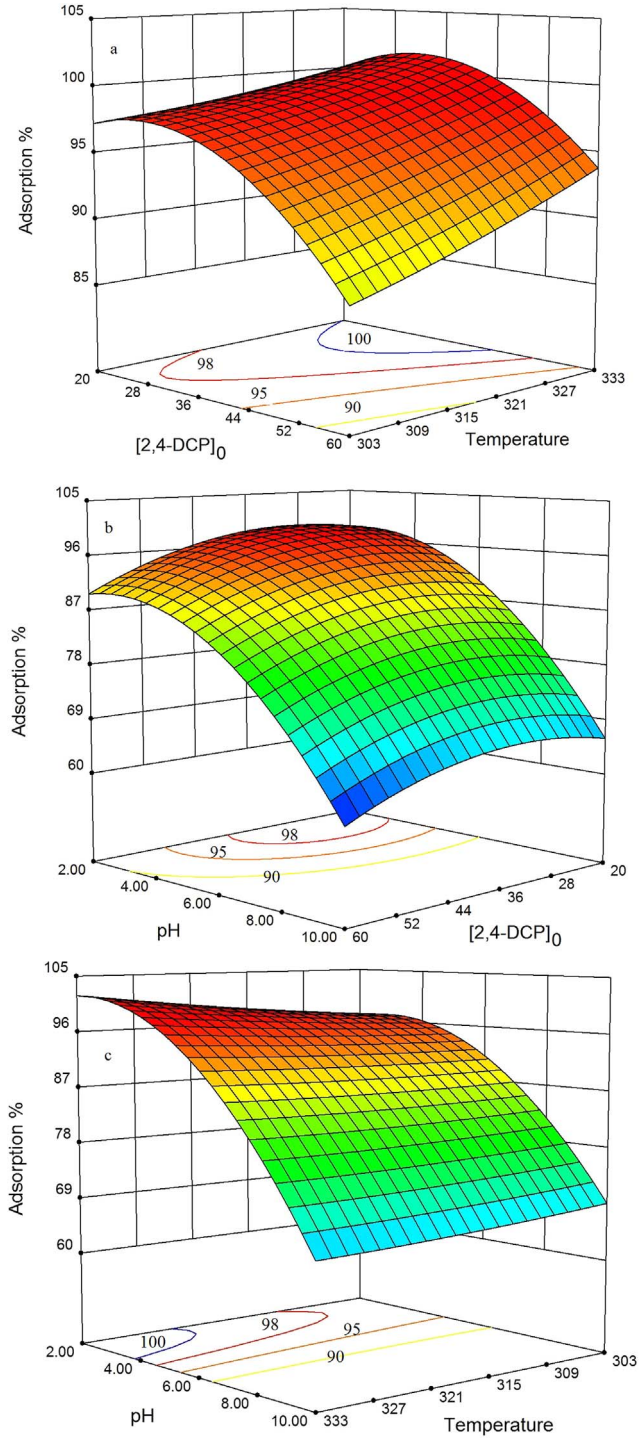

Fig. 4. Three-dimensional response surface plots showing the effects of significant interactions between a) initial 2,4-DCP concentration and temperature (pH = 3.00, t = 125 min) b) pH and initial 2,4-DCP concentration (T = 325 K, t = 125 min) c) pH and temperature ($[2,4\text{-DCP}]_0$ = 35 mg/L, t = 125 min).

concluded that at higher pH values there is an increasing electrostatic repulsion between the carbon fibers surface and dichlorophenate anions in solution [43]. Since the pH_{pzc} value of BC-A is 8.5, its surface was negatively charged at higher pH values, therefore repelling the anionic dichlorophenate. As the pH drops, higher percentage 2,4-DCP becomes neutral and the repulsion phenomenon is practically diminished, allowing for higher adsorption rates. Similar observations were reported by Oh et al. and Yuan et al. who found a negative correlation between 2,4-DCP sorption and pH, confirming that lower pH values may be favourable for the sorption of ionizable chlorophenols on biochars [44,45]. It is also possible that at very low pH values, the biochar's surface is surrounded by H_3O^+ ions which promote the interaction of chlorinated phenols with the biochar surface [42]. It is interesting to note that biochar can successfully remove 2,4-DCP from wastewaters, however this may not be necessarily the case in soils contaminated with the same substance. When Gu et al. applied biochar in 2,4-DCP contaminated soil, they found that the contaminant's biodegradation and mineralization was considerably reduced due to its strong sorption on the biochar's surface [46].

3.3. Application of equilibrium isotherms

Applying the experimental adsorption data points to known isotherms, allowed us to further investigate the interaction between 2,4-DCP and the biochar's surface. Two commonly used isotherm models were employed, namely the Langmuir and Freundlich models. The theoretical background and corresponding equations of these models have been described in detail elsewhere [26,37,41]. Briefly, the Langmuir isotherm assumes monolayer adsorption onto a surface containing a specific number of adsorption sites, whereas the Freundlich isotherm is an empirical model that describes adsorption on the basis that surfaces consist of adsorption sites of varying affinities (heterogeneous). Table 4 presents the values of the Langmuir and Freundlich parameters and a comparison with values obtained by other researchers. Both models provided an excellent fit for our data, indicating a combination of surface and multi-layer adsorption. The Langmuir equilibrium parameter R_L (or constant separation factor) can be calculated as follows:

$$R_L = \frac{1}{1 + bC_o} \quad (5)$$

Where, b is the adsorption binding constant (calculated from the slope of the Langmuir isotherm) and C_o the initial 2,4-DCP concentration. A value of R_L between 0 and 1 indicates favorable adsorption. Eq. (5) resulted in a value of 0.109 for the biochar used in this study, verifying the applicability of the Langmuir model. The adsorption capacity is comparable to the values obtained by other researchers who used biochars or other biomass-derived carbonaceous materials. However, it is well below the values obtained from activated materials and nanoporous adsorbents. With respect to the Freundlich equation, K_F and n are constants related to sorption capacity and sorption intensity, respectively. Both values compare favorably to those reported in the literature (Table 4).

3.4. Adsorption kinetics

The dynamics of the adsorption were investigated in terms of the order of the rate constant. The rate-controlling mechanisms of the adsorption process are commonly studied by applying the pseudo-first-order (Lagergren's model), pseudo-second-order, intra-particle diffusion and Bangham kinetic models. The theoretical details and corresponding models' equations can be found in previous works [26,47]. The properties and constants corresponding to each model are shown in Table 5. The pseudo-first order calculated q_e value was considerably different to the experimental value, whereas the correlation coefficient was lower compared to the respective pseudo-second order value. Additionally, the pseudo-second order calculated and experimental q_e values were in very good agreement, indicating that the process is mainly controlled by chemisorption and to a lesser extent by physical interactions. This conclusion comes in good agreement with earlier results reported in the literature [24,26,39,43,45]. Generally, it appears that many published papers agree on the kinetic model that best describes the adsorption of 2,4-DCP, regardless of adsorbent used.

The parameter C of the intra-particle diffusion model corresponds to the thickness of the boundary layer. If the value of C is zero, this means

Table 4
Comparison of the Langmuir and Freundlich isotherm parameters' values to those reported in literature.[a]

Langmuir parameters			Freundlich parameters			Adsorbent	Reference
q_{max} (mg g^{-1})	b	R^2	K_f	n	R^2		
17.51	0.204	0.990	2.76	1.2	0.998	Paper sludge/wheat husks biochar	This work
7.77	0.064	0.945	0.98	2.16	0.867	Anaerobic granular sludge	[42]
26.87	0.815	0.888	9.44	2.05	0.986	Microporous carbon fiber	[24]
10.69	0.035	0.946	0.302	0.79	0.965	$CaSO_4$-modified biochar	[41]
16.37	0.031	0.969	0.41	0.80	0.982	Hydroxyapatite/$CaSO_4$-modified biochar	[41]
372	0.170	0.999	55.1	2.01	0.905	Activated carbon fibers	[43]
46.9	8.235	0.998	0.409	1.78	0.972	Carbopack B	[25]
68.5	12.675	0.998	0.603	3.23	0.983	Vulcan XC-72	[25]
176.1	115.35	0.880	2.39	2.5	0.980	Peach stone activated carbon	[26]
90.8	0.059	0.981	8.19	1.79	0.986	Graphene oxide composite	[55]
450	0.002	0.660	1.90	0.57	0.958	Carbon nanotubes	[45]

[a] This table is indicative and any comparisons are subject to additional variables such as the biosorbent surface area and initial pH of the adsorbate solution.

Table 5
Parameters of the kinetic models applied.

Kinetic model	Parameter	Value
Pseudo-first order	q_e,experimental (mg g^{-1})	9.28
	q_e,calculated (mg g^{-1})	4.25
	k_A (min^{-1})	0.015
	R^2	0.968
Pseudo-second order	q_e,experimental (mg g^{-1})	9.28
	q_e,calculated (mg g^{-1})	9.55
	k_B (g mg^{-1} min^{-1})	0.011
	R^2	0.996
Intra-particle diffusion	k_{int} (mg g^{-1} $min^{-1/2}$)	0.23
	C (mg g^{-1})	6.10
	R^2	0.991
Bangham	α	0.469
	K_j	12.67
	R^2	0.817

that adsorption is exclusively controlled by the intra-particle diffusion mechanism. However, a C value of 6.1 and a high correlation coefficient indicate that the boundary layer effects are not negligible and co-exist with chemisorption. The Bangham kinetic model did not provide a satisfactory fit to the experimental data, thus confirming the observation that the process was not restricted by pore diffusion.

3.5. Comparison of different biochars on the adsorption of 2,4-DCP

Having optimized the process based on BC-A, the adsorption at equilibrium q_e of BC-B, BC-C and BC-D was determined at the same conditions used to measure the q_e for BC-A (0.1 g of adsorbent, C_0 = 40 mg L^{-1}, T = 328 K, pH = 2, t = 10–180 min). The adsorption capacities at equilibrium were 2.5, 1.57, and 2.96 mg g^{-1} for BC-B, BC-C and BC-D, respectively. These values are considerably lower compared to the 9.28 mg g^{-1} obtained with BC-A. These large differences may be explained by taking a closer look at all the potential sorption mechanisms and the biochars' properties (Table 1). The sorption mechanisms of organic substances on biochars and other carbonaceous materials are well-known and have been extensively reviewed. Researchers have determined that pore-filling, partitioning, hydrophobicity of biochar's surface, aromatic and cation-π interactions, electrostatic interactions and H-bonding could simultaneously occur [22,44,48,49].

The total surface area is closely connected to the average pore diameter and the biochars used in this study are essentially mesoporous materials whereas their micropore network is limited. If pore-filling was the dominant mechanism and the biochars were microporous, then the sample with the highest surface area (BC-D) would probably exhibit the highest adsorption %. For example, Yang et al. compared the adsorption of 2,4-DCP on five microporous zeolites and concluded that the exact micropore size played a very important role in the process, since the narrowest dimension of a 2,4-DCP molecule was measured as 0.482 nm [22]. Contrary to microporous materials, this molecule size would not be expected to restrict or promote the pore-filling process in mesoporous materials. Therefore, the lower surface area of BC-A (compared to BC-B and BC-D) cannot be correlated to the highest adsorption % under this hypothesis. Consequently, pore-filling is not the dominant adsorption mechanism and cannot account for the 2,4-DCP adsorption differences between the 4 samples. This conclusion is also supported by the results obtained from the kinetics investigation, where the Bangham model (pore-filling) did not provide a satisfactory fit.

The partitioning mechanism has been strongly correlated to the organic carbon present in biochars [48,50] and is characterized by concentration-independent, linear isotherms [51]. The carbon values reported for the biochars here, correspond to the sum of organic and inorganic (e.g. carbonates) carbon, therefore any conclusions with respect to the extent of partitioning cannot be drawn.

Hydrophobic interactions between the adsorbate and adsorbent may also promote sorption. Sorption of chlorophenols increases with the hydrophobicity of the adsorbates and that of the adsorbent [22]. The O/C ratio (Table 1) is indicative of the hydrophobicity of the biochar's surface. The lower this ratio is, the more aromatic and hydrophobic the biochar is, due to the larger degree of carbonization and loss of polar functional groups [50]. Therefore, BC-B appears to be the most hydrophobic, followed by BC-A and BC-D, whereas BC-C is the least hydrophobic. This trend does not account for the sorption capacities mentioned earlier, indicating that hydrophobic interactions solely are not the dominant mechanism.

Planar, aromatic compounds such as 2,4-DCP may also sorb to the biochar surface through a stable, non-covalent π-electron donor-acceptor mechanism, between an electron-withdrawing atom such as Cl and an area on the biochar surface with high density of π-electrons [43,48]. Biochars prepared at temperatures in the range of 500–700 °C (such as the ones used here) often have non-uniform charge distribution, therefore resulting in both π-electron hotspots and deficient surface areas [52]. Biochar surfaces with uniformly distributed π-electrons can only be achieved with complete carbonization of the biomass (> 1000 °C). The same conclusion was drawn by Peng et al. who studied the adsorption of antibiotics on two biochars and graphene. Although graphene had the lowest surface area and number of functional groups, it showed the strongest adsorption ability due to the dominant π-π interaction mechanism [53]. Additionally, biochars with high concentrations of Ca, K, and Mg may promote specific cation-π interactions and increase the adsorption of aromatic compounds [54]. The concentrations of these cations depend on the feedstock material

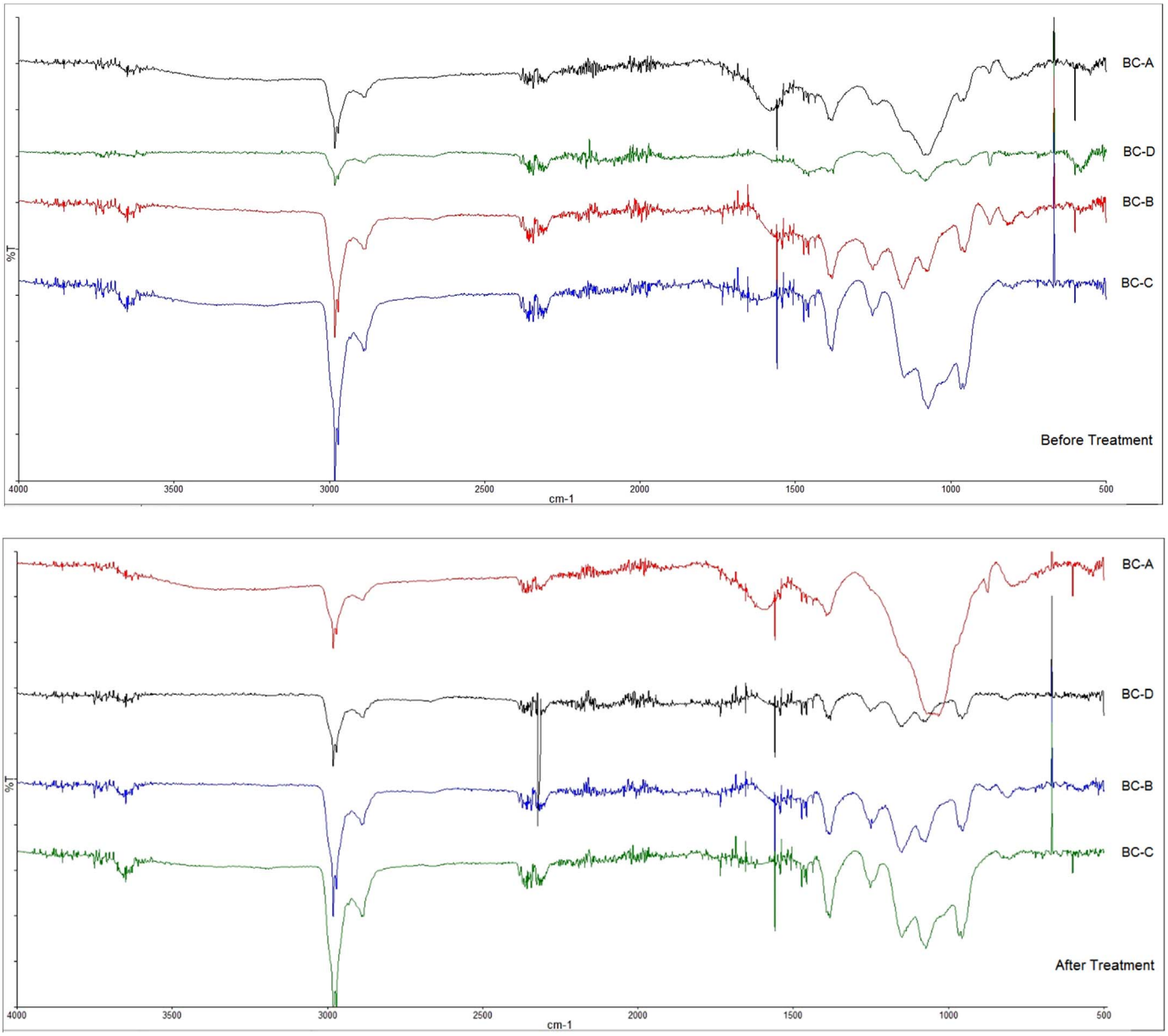

Fig. 5. FT-IR spectra of the biochar samples, before and after treatment.

and pyrolysis conditions. Overall, BC-A had the highest concentration of Ca and K, therefore this may partly account for the highest equilibrium adsorption among the 4 samples. However, further analysis of the ash content is required to determine the effect of minerals such as SiO_2 and Al_2O_3 in adsorption.

The electrostatic interaction between 2,4-DCP and BC-A is pH-dependent and was discussed in Section 3.3. It has been established that in most systems with biochars and ionizable contaminants, electrostatic interactions play a major role in adsorption [44,48]. All biochars used in this study were essentially alkaline and their pH_{pzc} values were similar (Table 1). Therefore, it is expected that the same mechanism would apply to all biochar samples but at the same time it cannot explain the differences in the q_e values. Hydrogen bonding may also occur between polar groups on the biochar surface and electronegative atoms on 2,4-DCP, although Cl does not generally form H bonds due to its large atomic radius. FT-IR spectra obtained for biochar samples before and after treatment was depicted in Fig. 5. Bare biochar structures showed similar spectra in the functional group region. The bands at approximately 3600 cm^{-1} are attributed to −OH (free) stretching from the hydroxyl groups of biochars. It is possible to see the aromatic and aliphatic −CH stretching vibrations between 3040 and 2800 cm^{-1}. Also the C=C stretching vibration of the aromatic rings was shown at 1559 cm^{-1}. The band spectrum at 1600 cm^{-1} was assigned to the stretching vibration of carbonyl- C=O. In the finger-print region, the well-defined bands in the range of 1300–900 cm^{-1} were evidence to −C−O groups such as ether, ester or phenol linkage. The bands at 1252 cm^{-1} attributing to the phenolics −OH stretching vibration. The broad peaks were observed around 1150 and 1050 cm^{-1} corresponds to tertiary and primary alcohols C−O stretch, respectively. Infrared spectra of the biochars after treatment showed no significant changes compared to the bare. Therefore, the difference in adsorption capacities cannot be attributed to any differences in the moieties present on the biochars' surface.

4. Conclusions

The use of unprocessed and unmodified paper sludge/wheat husks biochar for the adsorption of 2,4-DCP showed promising behavior. The

highest experimental adsorption % achieved was 98.85, at an initial contaminant concentration of 40 mg L^{-1}, temperature of 333 K, pH 2 and treatment time of 120 min. Optimization of the process using a Box-Behnken design, predicted an optimum adsorption % of 99.95, at 40.28 mg L^{-1} 2,4-DCP concentration, pH 2.81, temperature 326 K, and treatment time of 143 min. With a q_{max} of 17.51 mg g^{-1}, BC-A compared favorably to other biochars and natural adsorbents reported in the literature but well below activated materials. The isotherm and kinetic model studies indicated that surface and multi-layer pH-dependent chemisorption was the dominant mechanism. Comparison of BC-A to other biochars with higher surface area supported this conclusion and promoted the theory that electrostatic interactions play a more important role than pore-filling and diffusion processes. Additionally, it appears that the presence of cations such as Ca and K correlate positively to the adsorption of 2,4-DCP on biochars. Further characterization work is required to strengthen this claim and help develop engineered biochars for chlorophenol adsorption. Therefore, it may be preferable to focus on biomasses with high Ca and K concentrations, rather than trying to adjust the pyrolysis conditions so that a high surface area biochar is obtained.

Acknowledgments

The authors would like to thank Hans-Peter Schmidt (Ithaka Institute, Ayent, Valais, Switzerland) and Francesco Tortorici (Olympic Biochar, Port Townsend, United States) for providing some of the biochar characterization values of Table 1.

References

[1] L.W.B. Olaniyan, N. Mkwetshana, A.I. Okoh, Triclosan in water, implications for human and environmental health, Springerplus 5 (2016) 1639–1656.
[2] J.C.H. Ho, C.D. Hsiao, K. Kawakami, W.K.F. Tse, Triclosan (TCS) exposure impairs lipid metabolism in zebrafish embryos, Aquat. Toxicol. 173 (2016) 29–35.
[3] G.S. Dhillon, S. Kaur, R. Pulicharla, S.K. Brar, M. Cledón, M. Verma, et al., Triclosan: current status, occurrence, environmental risks and bioaccumulation potential, Int. J. Environ. Res. Public Health. 12 (2015) 5657–5684.
[4] J. Chen, R. Qu, X. Pan, Z. Wang, Oxidative degradation of triclosan by potassium permanganate: kinetics, degradation products, reaction mechanism, and toxicity evaluation, Water Res. 103 (2016) 215–223.
[5] G. Bedoux, B. Roig, O. Thomas, V. Dupont, B. Le Bot, Occurrence and toxicity of antimicrobial triclosan and by-products in the environment, Environ. Sci. Pollut. Res. 19 (2012) 1044–1065.
[6] E. Geiger, R. Hornek-Gausterer, M.T. Saçan, Single and mixture toxicity of pharmaceuticals and chlorophenols to freshwater algae *Chlorella vulgaris*, Ecotoxicol. Environ. Saf. 129 (2016) 189–198.
[7] H. Ensley, J.T. Barber, M.A. Polito, A.I. Oliver, Toxicity and metabolism of 2,4-dichlorophenol by the aquatic angiosperm *Lemna gibba*, Environ. Toxicol. Chem. 13 (1994) 325–331.
[8] A. Shaukat, G. Liu, Z. Li, D. Xu, Y. Huang, H. Chen, Toxicity of five phenolic compounds to brine shrimp *Artemia sinica* (Crustacea: Artemiidae), J. Ocean Univ. China 13 (2014) 141–145.
[9] A.M. Aker, D.J. Watkins, L.E. Johns, K.K. Ferguson, O.P. Soldin, L.V. Anzalota Del Toro, et al., Phenols and parabens in relation to reproductive and thyroid hormones in pregnant women, Environ. Res. 151 (2016) 30–37.
[10] J. Guo, C. Wu, S. Lv, D. Lu, C. Feng, X. Qi, et al., Associations of prenatal exposure to five chlorophenols with adverse birth outcomes, Environ. Pollut. 214 (2016) 478–484.
[11] R.P. Pohanish, Sittig's Handbook of Toxic and Hazardous Chemicals and Carcinogens, Elsevier Science, 2011.
[12] J. Zhou, H. Chen, Q. Chen, Z. Huang, Bimetallic Au-decorated Pd catalyst for the liquid phase hydrodechlorination of 2,4-dichlorophenol, Appl. Surf. Sci. 387 (2016) 588–594.
[13] X. Cui, W. Zuo, M. Tian, Z. Dong, J. Ma, Highly efficient and recyclable Ni MOF-derived N-doped magnetic mesoporous carbon-supported palladium catalysts for the hydrodechlorination of chlorophenols, J. Mol. Catal. A Chem. 423 (2016) 386–392.
[14] J. Xu, J. Tang, S.A. Baig, X. Lv, X. Xu, Enhanced dechlorination of 2,4-dichlorophenol by Ni/Fe-Fe_3O_4 nanocomposites, J. Environ. Sci. 48 (2016) 92–101.
[15] Y. Qian, J. Zhang, Y. Zhang, J. Chen, X. Zhou, Degradation of 2,4-dichlorophenol by nanoscale calcium peroxide: implication for groundwater remediation, Sep. Purif. Technol. 166 (2016) 222–229.
[16] M. Kurian, C. Kunjachan, A. Sreevalsan, Catalytic degradation of chlorinated organic pollutants over $Ce_xFe_{1-x}O_2$ (x: 0, 0. 25, 0. 5, 0. 75, 1) nanocomposites at mild conditions, Chem. Eng. J. 308 (2017) 67–77.
[17] X. Li, M. Zhou, Y. Pan, L. Xu, Pre-magnetized Fe°/persulfate for notably enhanced degradation and dechlorination of 2, 4-dichlorophenol, Chem. Eng. J. 307 (2017) 1092–1104.
[18] P. Devi, U. Das, A.K. Dalai, In-situ chemical oxidation: principle and applications of peroxide and persulfate treatments in wastewater systems, Sci. Total Environ. 571 (2016) 643–657.
[19] C. Zhang, M. Zhou, G. Ren, X. Yu, L. Ma, J. Yang, et al., Heterogeneous electro-fenton using modified iron-carbon as catalyst for 2,4-dichlorophenol degradation: influence factors, mechanism and degradation pathway, Water Res. 70 (2015) 414–424.
[20] E. Bilgin Simsek, Solvothermal synthesized boron doped TiO_2 catalysts: photocatalytic degradation of endocrine disrupting compounds and pharmaceuticals under visible light irradiation, Appl. Catal. B Environ. 200 (2017) 309–322.
[21] X. Song, Q. Shi, H. Wang, S. Liu, C. Tai, Z. Bian, Preparation of Pd-Fe/graphene catalysts by photocatalytic reduction with enhanced electrochemical oxidation-reduction properties for chlorophenols, Appl. Catal. B: Environ. 203 (2017) 442–451.
[22] H. Yang, Y. Hu, H. Cheng, Sorption of chlorophenols on microporous minerals: mechanism and influence of metal cations, solution pH, and humic acid, Environ. Sci. Pollut. Res. (2016) 1–15.
[23] K. Ortiz-Martínez, P. Reddy, W.A. Cabrera-Lafaurie, F.R. Román, A.J. Hernández-Maldonado, Single and multi-component adsorptive removal of bisphenol A and 2,4-dichlorophenol from aqueous solutions with transition metal modified inorganic-organic pillared clay composites: effect of pH and presence of humic acid, J. Hazard. Mater. 312 (2016) 262–271.
[24] E. Bilgin Simsek, I. Novak, O. Sausa, D. Berek, Microporous carbon fibers prepared from cellulose as efficient sorbents for removal of chlorinated phenols, Res. Chem. Intermed. (2016) 1–20.
[25] K. Kuśmierek, M. Szala, A. Świątkowski, Adsorption of 2,4-dichlorophenol and 2,4-dichlorophenoxyacetic acid from aqueous solutions on carbonaceous materials obtained by combustion synthesis, J. Taiwan Inst. Chem. Eng. 63 (2016) 371–378.
[26] E. Bilgin Simsek, B. Aytas, D. Duranoglu, U. Beker, A.W. Trochimczuk, A comparative study of 2-chlorophenol 2,4-dichlorophenol, and 2,4,6-trichlorophenol adsorption onto polymeric, commercial, and carbonaceous adsorbents, Desalin. Water Treat. 57 (2016) 9940–9956.
[27] Z.N. Garba, A.A. Rahim, Evaluation of optimal activated carbon from an agricultural waste for the removal of para-chlorophenol and 2,4-dichlorophenol, Process Saf. Environ. Prot. 102 (2016) 54–63.
[28] S.M. Anisuzzaman, C.G. Joseph, D. Krishnaiah, A. Bono, E. Suali, S. Abang, et al., Removal of chlorinated phenol from aqueous media by guava seed (*Psidium Guajava*) tailored activated carbon, Water Resour. Ind. 16 (2016) 29–36.
[29] A. Alsbaiee, B.J. Smith, L. Xiao, Y. Ling, D.E. Helbling, W.R. Dichtel, Rapid removal of organic micropollutants from water by a porous β-cyclodextrin polymer, Nature 529 (2016) 190–194.
[30] M. Laghari, R. Naidu, B. Xiao, Z. Hu, M.S. Mirjat, M. Hu, et al., Recent developments in biochar as an effective tool for agricultural soil management: a review, J. Sci. Food Agric. 96 (2016) 4840–4849.
[31] Y. Ding, Y. Liu, S. Liu, Z. Li, X. Tan, X. Huang, et al., Biochar to improve soil fertility. a review, Agron. Sustain. Dev. 36 (2016).
[32] M.I. Inyang, B. Gao, Y. Yao, Y. Xue, A. Zimmerman, A. Mosa, et al., A review of biochar as a low-cost adsorbent for aqueous heavy metal removal, Crit. Rev. Environ. Sci. Technol. 3389 (2015) 406–433.
[33] T. Xie, K.R. Reddy, C. Wang, E. Yargicoglu, K. Spokas, Characteristics and applications of biochar for environmental remediation: a review, Crit. Rev. Environ. Sci. Technol. 45 (2014) 939–969.
[34] M. Ahmad, A.U. Rajapaksha, J.E. Lim, M. Zhang, N. Bolan, D. Mohan, et al., Biochar as a sorbent for contaminant management in soil and water: a review, Chemosphere 99 (2014) 19–23.
[35] G. Newcombe, R. Hayes, M. Drikas, Granular activated carbon: importance of surface properties in the adsorption of naturally occurring organics, Colloids Surf. A Physicochem. Eng. Aspects 78 (1993) 65–71.
[36] E. Agrafioti, D. Kalderis, E. Diamadopoulos, Arsenic and chromium removal from water using biochars derived from rice husk, organic solid wastes and sewage sludge, J. Environ. Manag. 133 (2014) 309–314.
[37] M. Şener, B. Kayan, S. Akay, B. Gözmen, D. Kalderis, Fe-modified sporopollenin as a composite biosorbent for the removal of Pb^{2+} from aqueous solutions, Desalin. Water Treat. 3994 (2016) 1–19.
[38] K. Mkadmini Hammi, M. Hammami, C. Rihouey, D. Le Cerf, R. Ksouri, H. Majdoub, Optimization extraction of polysaccharide from Tunisian *Zizyphus lotus* fruit by response surface methodology: composition and antioxidant activity, Food Chem. 212 (2016) 476–484.
[39] F. Ren, R. Zhang, W. Lu, T. Zhou, R. Han, S. Zhang, Adsorption potential of 2,4-dichlorophenol onto cationic surfactant-modified phoenix tree leaf in batch mode, Desalin Water Treat. 57 (2016) 6333–6346.
[40] A. Bhatnagar, A.K. Minocha, Adsorptive removal of 2,4-dichlorophenol from water utilizing *Punica granatum* peel waste and stabilization with cement, J. Hazard. Mater. 168 (2009) 1111–1117.
[41] A.H. Alamin, L. Kaewsichan, Equilibrium and kinetic studies of sorption of 2, 4-dichlorophenol onto 2 mixtures: bamboo biochar plus calcium sulphate (BC) and hydroxyapatite plus bamboo biochar plus calcium sulphate (HBC), in a fluidized bed circulation column, Pol. J. Chem. Technol. 18 (2016) 59–67.
[42] R. Gao, J. Wang, Effects of pH and temperature on isotherm parameters of chlorophenols biosorption to anaerobic granular sludge, J. Hazard. Mater. 145 (2007) 398–403.
[43] J.P. Wang, H.M. Feng, H.Q. Yu, Analysis of adsorption characteristics of 2,4-dichlorophenol from aqueous solutions by activated carbon fiber, J. Hazard. Mater. 144 (2007) 200–207.

[44] S.Y. Oh, Y.D. Seo, Sorption of halogenated phenols and pharmaceuticals to biochar: affecting factors and mechanisms, Environ. Sci. Pollut. Res. 23 (2016) 951–961.
[45] H. Yuan, Q. liang You, L.J. Song, G. ying Liao, H. Xia, D.S. Wang, Preparation of carbon nanotubes/porous polyimide composites for effective adsorption of 2,4-dichlorophenol, RSC Adv. 6 (2016) 95825–95835.
[46] J. Gu, W. Zhou, B. Jiang, L. Wang, Y. Ma, H. Guo, et al., Effects of biochar on the transformation and earthworm bioaccumulation of organic pollutants in soil, Chemosphere 145 (2016) 431–437.
[47] A.A. Inyinbor, F.A. Adekola, G.A. Olatunji, Kinetics, isotherms and thermodynamic modeling of liquid phase adsorption of Rhodamine B dye onto *Raphia hookerie* fruit epicarp, Water Resour. Ind. 15 (2016) 14–27.
[48] M. Inyang, E. Dickenson, The potential role of biochar in the removal of organic and microbial contaminants from potable and reuse water: a review, Chemosphere 134 (2015) 232–240.
[49] X. Tan, Y. Liu, G. Zeng, X. Wang, X. Hu, Y. Gu, et al., Application of biochar for the removal of pollutants from aqueous solutions, Chemosphere 125 (2015) 70–85.
[50] G.N. Kasozi, A.R. Zimmerman, P. Nkedi-Kizza, B. Gao, Catechol and humic acid sorption onto a range of laboratory-produced black carbons (biochars), Environ. Sci. Technol. 44 (2010) 6189–6195.
[51] B. Chen, D. Zhou, L. Zhu, Transitional adsorption and partition of non-polar and polar aromatic contaminants by biochars of pine needles with different pyrolytic temperatures, Environ. Sci. Technol. 42 (2008) 5137–5143.
[52] D. Zhou, J.J. Pignatello, Characterization of aromatic compound sorptive interactions with black carbons (charcoal) assisted by graphite as a model, Environ. Sci. Technol. 39 (2005) 2033–2041.
[53] B. Peng, L. Chen, C. Que, K. Yang, F. Deng, X. Deng, et al., Adsorption of antibiotics on graphene and biochar in aqueous solutions induced by π-π interactions, Sci. Rep. 6 (2016) 31920.
[54] S.Y. Oh, J.G. Son, P.C. Chiu, Biochar-mediated reductive transformation of nitro herbicides and explosives, Environ. Toxicol. Chem. 32 (2013) 501–508.
[55] H. Yan, Q. Du, H. Yang, A. Li, R. Cheng, Efficient removal of chlorophenols from water with a magnetic reduced graphene oxide composite, Sci. China Chem. 59 (2016) 350–359.